Iraqi Journal of Science, 2024, Vol. 65, No. 11, pp: 6502-6512
DOI: 10.24996/ijs.2024.65.11.26

ISSN: 0067-2904

Study of Structure and Morphology of Chromium Nanoparticles Prepared by Pulse Laser Ablation and its Effect on Bacteria

Raghad T. Ahmed[1] , Ala F. Ahmed[2*], Kadhim A. Aadim[1]
[1]*Department of physics, College of Science, University of Baghdad, Baghdad, Iraq*
[2]*Department of Astronomy & Space, College of Science, University of Baghdad, Baghdad, Iraq.*

Received: 20/1/2023 Accepted: 4/9/2023 Published: 30/11/2024

Abstract

The study investigated the antibacterial properties of chromium nanoparticles using Pulse laser ablation technology. The nanoparticles were produced using a Q-switched Nd:YAG pulsed laser of 532 nm and pulsed laser energies ranging from 400mJ to 700mJ at a frequency of 6 Hz. The properties of the nanoparticles were characterized using various techniques, including XRD, AFM, SEM, and EDS, at laser energies of 400 and 700 mJ. The resulting chromium powder exhibited a crystalline structure, with average crystalline sizes of 42.25 and 52.53 nm for laser energies of 400 and 700 mJ, respectively. EDX analysis revealed the presence of chromium, carbon, and oxygen at different concentrations for both energy levels. FE-SEM images showed the shape and aggregation of the nanoparticles, with average diameters of 99.06 and 115.6 nm for laser energies of 400mJ and 700 mJ, respectively. The antibacterial properties of chromium nanoparticles were tested on Staphylococcus aureus and Escherichia coli bacteria. The number of bacteria colonies killed varied at different laser energy levels between 400 and 700 mJ. Nevertheless, complete eradication of Escherichia coli was achieved specifically at a laser energy level of 700 mJ.

Keywords: Pulse laser ablation (PLA), Nanoparticles (NPs), Chromium (Cr), Staphylococcus aurous bacteria, Escherichia coli bacteria

دراسة الخصائص الهيكلية والتشكيلية لجسيمات الكروم النانوية بواسطة الاستئصال بالليزر النبضي وتأثيره على بكتيريا

رغدة طلال احمد[1] , الاء فاضل احمد[2]* , كاظم عبد الواحد عادم[1]
[1] قسم الفيزياء,كلية العلوم ,جامعة بغداد ,بغداد ,العراق
[2] قسم الفلك والفضاء,كلية العلوم ,جامعة بغداد,بغداد,العراق

الخلاصة

تم تحضير الجسيمات النانوية للكروم بواسطة الاستئصال بالليزر النبضي باستخدام ليزر نابض Nd: YAG ذو طول موجي أساسي يبلغ 532 نانومتر عند طاقات مختلفة من (400–700) ملي جول وتردد ثابت (6 هرتز). تمت دراسة الخصائص للجسيمات النانوية باستخدام تقنيات مختلفة ، XRD ، و AFM ، و

*Email: ala.ahmed@sc.uobaghdad.edu.iq

SEM ، وEDX ، بطاقات ليزر تبلغ 400 و 700 مللي جول ، وأظهر مسحوق الكروم الناتج بنية بلورية ، بمتوسط أحجام بلورية 42.25 و 52.53 نانومتر لطاقات الليزر 400 و 700 مللي جول ، على التوالي. كشف تحليل EDX عن وجود الكروم والكربون والأكسجين بتركيزات مختلفة لكلا مستويي الطاقة. أظهرت صور
FE-SEM شكل وتجمع الجسيمات النانوية بمتوسط أقطار 99.06 و 115.6 نانومتر لطاقات الليزر 400ملي جول و700ملي جول على التوالي ، وتم تقييم التأثيرات المضادة للبكتيريا لجسيمات الكروم النانوية على نوعين مختلفين من البكتيريا ، ولوحظ أن عدد مستعمرات البكتيريا التي تم قتلها يختلف لكل مستوى طاقة ليزر يتراوح من 400 إلى 700 ملي جول. ومع ذلك ، فقد وجد أن البكتيريا الأشريكية القولونية قد تم القضاء عليها تمامًا عند طاقة ليزر 700 ملي جول.

1. Introduction.

Plasma is a near-neutral gas consisting of positively and negatively charged particles that collide or ionize neutral particles [1,2]. There are many applications of plasma, such as optical reagents, optoelectronic devices, biomedical, studying the Earth's ionosphere, solar cells, and other applications[3-7].

Laser ablation is one of the most effective physical processes for producing nano-particles. The procedure involves using intense laser radiation to ablate a solid target, resulting in the ejection of the target's contents and the production of nanostructures. When performed in a vacuum or residual gas, nano-clusters can form on a substrate placed at a distance from the target, creating a nanostructure film. This technology is used to remove materials from a solid surface by utilizing the energy of the absorbed laser, causing the material to evaporate and convert to plasma when the flow rate is high[8-12].

Pulse laser ablation (PLA) is a laser-induced ejection of macroscopic volumes of material from the surface of a solid caused by a short, intense laser pulse; it is known as laser ejection process. Although it is prevalent in many technology sectors, it is not widely used[13]. Laser ablation technology is defined as removing matter from the surface of a target through strong laser irradiation. The laser causes electrons from the conduction band in metals to condense by heating them to high temperatures. The heated electron gas excites phonons in the lattice and equilibrates on a picosecond timescale, resulting in a state of equilibrium [14-17].

Staphylococcus aureus is a gram-positive, opportunistic pathogen that has acquired virulence characteristics from its environment. One of the primary functions of its network of virulence factors is to detect environmental changes and respond by adjusting the production of virulence factors necessary for survival in the host. These virulence factors include cell surface adhesives, enzymes, and extracellular toxins, which aid in the bacterium's survival and proliferation within the host. By altering the production of these virulence factors, S. aureus can adapt to changes in its environment and ensure its survival in the host [11].

Escherichia coli is gram-negative bacteria commonly found in the normal colonic flora. It belongs to the Enterobacteriaceae family, composed of facultative bacteria that can survive in aerobic and anaerobic conditions. Although E. coli is typically harmless, it can potentially cause opportunistic infections. They can ferment glucose, reduce nitrates to nitrites, and are oxidase negative. Although most types of E. coli are safe and live in the digestive systems of both humans and animals, some strains can cause severe anaemia or kidney failure, which

can be fatal. Other strains of E. coli can cause urinary tract infections or other infections[18,19].

The goal of the research is to investigate the structural and morphological properties of chromium, as well as to determine its crystal size using XRD. Additionally, the study aims to examine how pulsed laser ablation affects bacteria.

2. Materials and methods.

2.1 Synthesis of Cr nanoparticles.

In this study, a Cr solid disc was prepared by pressing 2 grams of Cr powder using a hydraulic piston press (type SPECIAL) for 15 minutes. The disc was placed in a small beaker and covered with 4 ml of distilled water. The beaker was positioned on the base of a laser holder, and a pulse laser with a wavelength of 532 nm and 200 shots and varying laser energies (400 mJ and 700 mJ) was directed at the target element (the Cr disc), as shown in Figure 1. The interaction between the laser and the target element resulted in the formation nanomaterial, indicated by the change in the color of the distilled water.

2.2 Treatment of bacteria.

In the experiment, the solid disc of the Cr target was placed in a beaker, to which the best serial dilution of bacteria was added until the solid disc was completely covered. The disc was then bombarded by laser of different energies of (400-700) mJ at a wavelength of 532 nm. The ablation liquid was cultured on nutrient agar by the striking method.

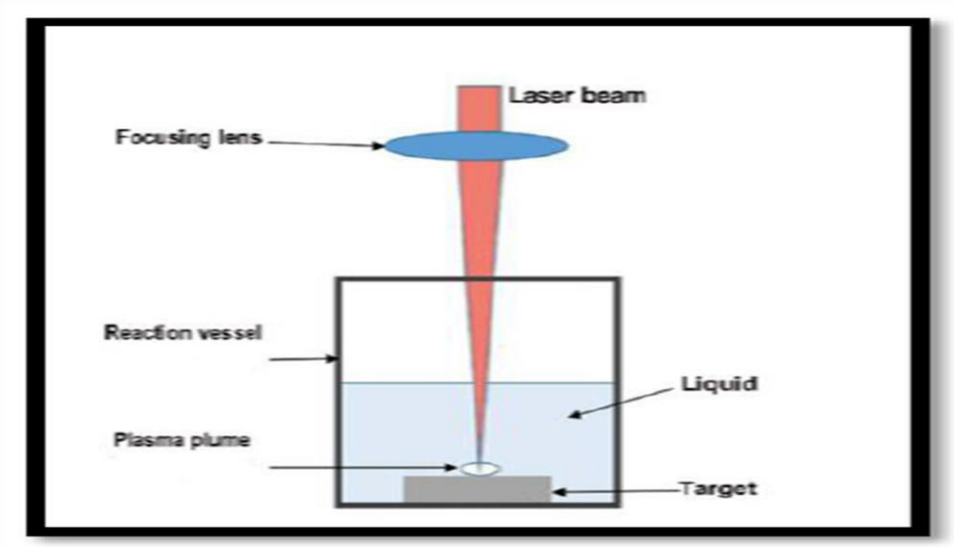

Figure 1: Schematic diagram of pulsed laser ablation in a liquid system

3 Result and Discussion.

3.1 X-ray Diffraction Analysis (XRD)

The crystal structure, direction, and particle size of a substance can all be identified by X-ray diffraction, a potent non-destructive technique for material analysis. Debye- Scherrer equation is used to determine the particle dimension (D) in a polycrystalline film: [20, 21].

$$D = \frac{K\lambda}{\beta COS\theta} \quad (1)$$

Where: β is the full width at half maximum (in radians) of the peak,θ is the Bragg angle .The source of the X-radiation was Cu (ka) with wavelength equal to 1.5406A^{o} .

The XRD pattern was recorded at a 2θ° angle ranging from 20° to 80° for the Cr powder, as shown in Figure (2). These results agree with the standard model (JCPDS No. 00-006-0694) for pure face-centered cubic phase Chromium nanoparticles. By comparing the Cr diffraction angles 2θ° with the JCPDS card number in the literature, X-ray diffraction (XRD) demonstrates the nature of the crystal structure of the pure Cr powder and Cr nanoparticles.

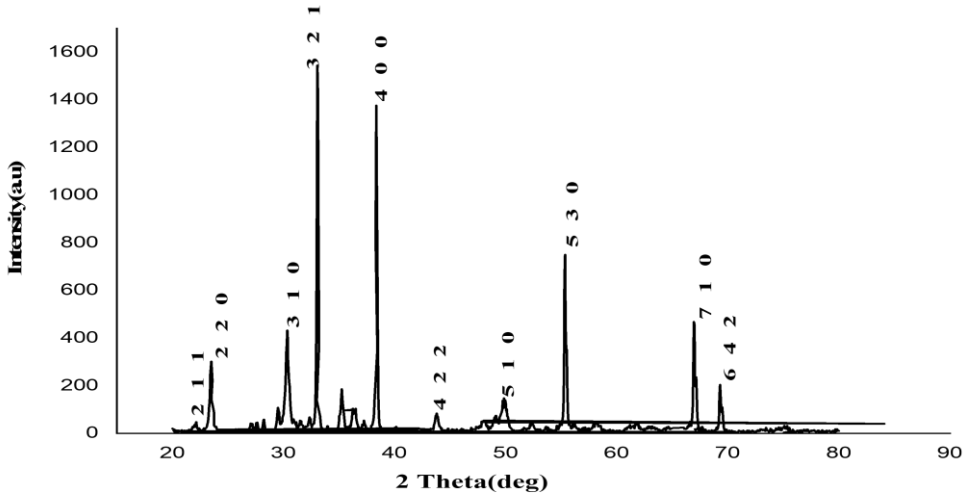

Figure 2: XRD pattern of Cr powder

The Debye-Scherrer equation was used to determine the crystalline size of chromium nanoparticles synthesized with laser energies of 400 mJ and 700 mJ. The structural parameters of the Chromium nanoparticles are provided in Table (1). Figures (3) and (4) display the corresponding XRD spectra. These spectra indicate that the chromium nanoparticle membranes have a polycrystalline and cubic crystal structure. It is evident that there are variations between the chromium films, which can be attributed to the different laser energies used during the deposition process for each film. Specifically, the average crystal size of the film synthesized with energy of 400 mJ was measured to be 42.25 nm, while the film synthesized with energy of 700 mJ exhibited an average crystal size of 52.53 nm. The observed increase in crystal growth can be attributed to the higher energy of the laser pulse used during the deposition process. This behavior agree with that reported by Wang and Nie[22]and de Haan[23].

Table 1 Structural parameters of Cr nanoparticles synthesized by Nd: YAG laser at energy of 400mJ and 700 mJ.

E(mj)	2 theta	FWHM(nm)	Crystallite size (nm)	Average C.S (nm)	hkl
400mJ	21.509	0.1476	54.76402	42.25	(3 1 1)
	25.376	0.246	33.0893		(2 2 0)
	38.217	0.1476	56.93948		(4 0 0)
	44.418	0.1968	43.58513		(4 2 2)
	55.938	0.393	22.87882		(5 3 0)
700mJ	21.389	0.1476	54.75316	52.53	(3 1 1)
	25.629	0.1476	55.1764		(2 2 0)
	38.389	0.1476	56.96917		(4 0 0)
	44.394	0.246	34.86512		(4 2 2)
	55.886	0.1476	60.9025		(5 3 0)

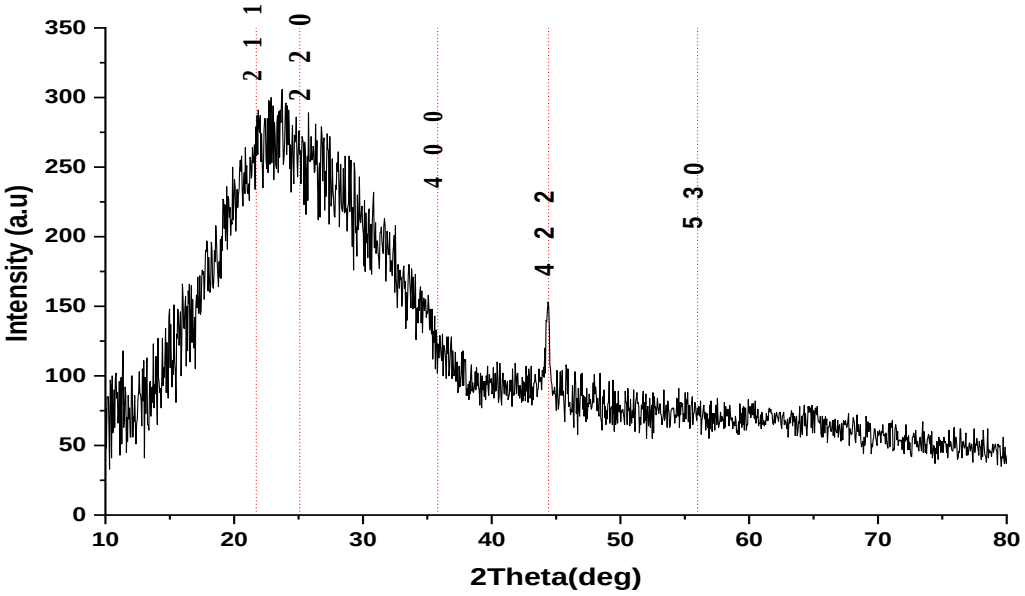

Figure 3: X-ray diffraction spectra of a Cr nanostructure produced by laser at energy of (400mJ)

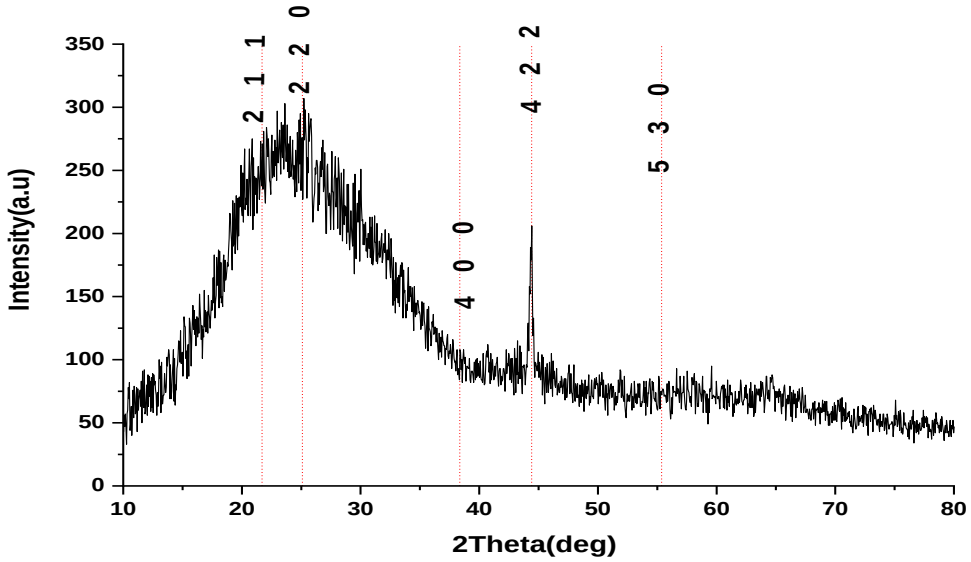

Figure 4 : X-ray diffraction spectra of a Cr nanostructure produced by laser at energy of(700mJ)

3.2 Atomic Force Microscope Analysis (AFM)

Atomic force microscopy (AFM) is a commonly employed technique for examining surface microstructure and quantifying surface topography. Its operation is based on the measurement of attractive or repulsive forces between a cantilever-tipped probe and the sample, while maintaining a constant height[14]. Figures (5) and (6) display three-dimensional images showing irregular surface or pyramid shape and a homogeneous membrane. The results indicated that all atoms have a particle size in the nano-scale range,

with an average roughness of 1.011nm, an average diameter of 99.06 nm, a root mean square of 1.413 nm at 400 mJ energy, and an average roughness of 2.605 nm, an average diameter of 115.6 nm, and a root mean square of 3.140nm at 700 mJ energy. One can notice from this figure that as the pulse laser energy increases, the granular diameter increases. This increase is due to two reasons: when the energy of the pulse increases, large granules are produced, and the second is that the increase in the energy of the pulse allows small grains to agglomerate, and thus coalescence occurs, resulting in the production of large granules, and this will lead to an increase in the roughness of the surface and the diameter of the grain size[17, 24].

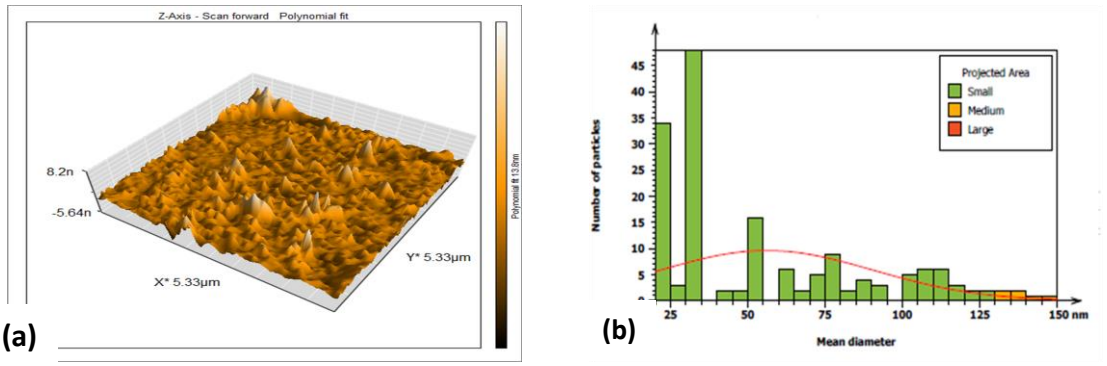

Figure 5: 3D AFM images of Cr NPs prepared by PLA (a) with 400 mJ laser energy and (b)granularity accumulation distribution

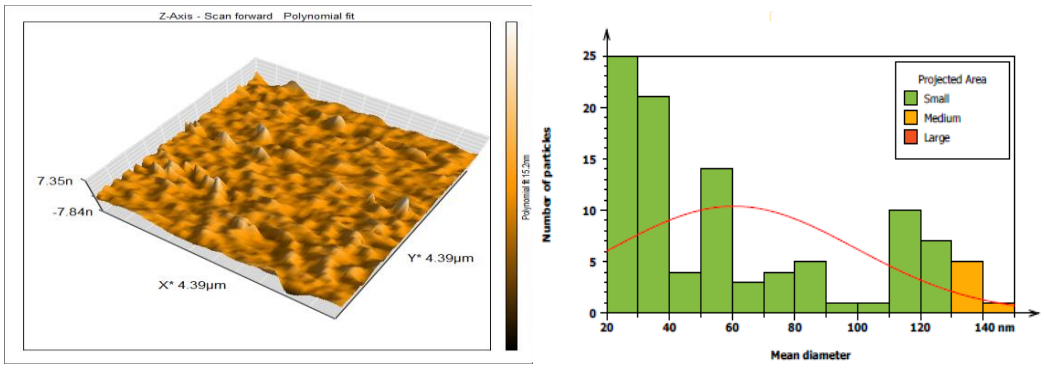

Figure 6: 3D AFM images Cr NPs prepared by PLA (a) with 700 mJ laser energy and (b) granularity accumulation distribution

3.3 Analysis of Cr by Field Emission Scanning Electron Microscopy (FE-SEM) and Energy Dispersive X-ray (EDX)

Field emission scanning electron microscopy (FE-SEM) is an essential instrument for the characterization of nanoscale materials. FE-SEM can achieve spatial resolutions of less than one nanometer because it images samples using electrons rather than photons. [15]. Figures 7 and 8 depict the surface morphology of chromium nanoparticles prepared using laser-induced plasma at 400 mJ and 700 mJ, respectively. The images show a variety of shapes and sizes of the synthesized chromium nanoparticles, with some spaces between them that become denser as the laser energy increases from 400 mJ to 700 mJ. The nanoparticles

have a spherical or semi-spherical shape, as seen in the FE-SEM images[25]. However, agglomeration of the nanoparticles can also be observed due to the attractive forces between them. Overall, the images demonstrate the successful formation of nanostructured chromium particles using the employed laser energies [26].

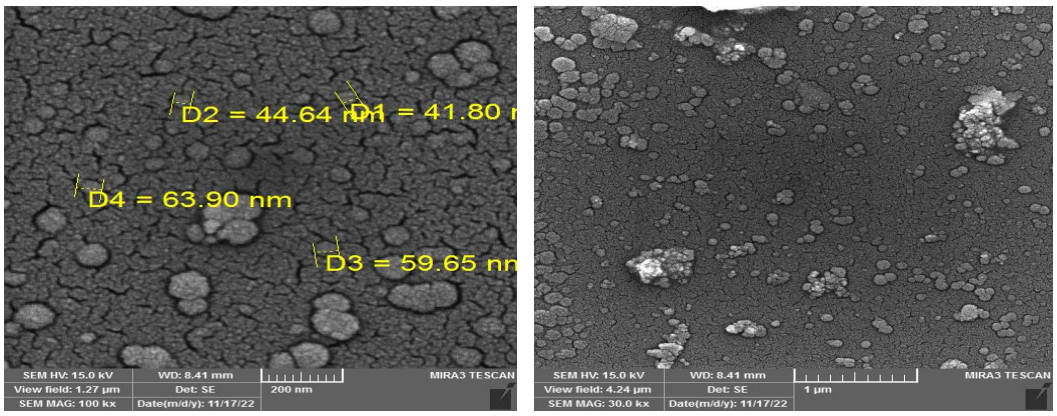

Figure 7: FE-SEM images of Cr NPs measure range (200nm and 1 µm) with laser energy of 400mJ

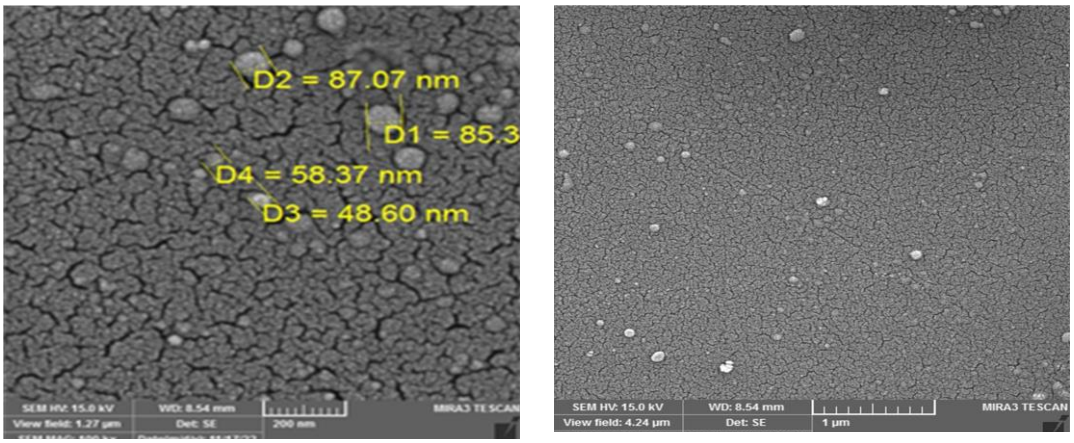

Figure 8: FE-SEM images of Cr NPs measurement at range (200nm and 1 µm) with laser energy of 700mJ

The concentration of elements in a chromium nanoparticle solution was determined using Energy-dispersive X-ray spectroscopy (EDX), which confirmed the presence of **c**hromium. The chemical composition of the produced Cr samples was also analyzed using EDX, which showed peaks associated with Cr, C, and O elements and no additional impurities. The study found that increasing the laser energy resulted in the production of exceedingly small particles. The percentages of Cr, C, and O components were determined for the two laser energies of 400 mJ and 700 mJ, as shown in Figure 9.

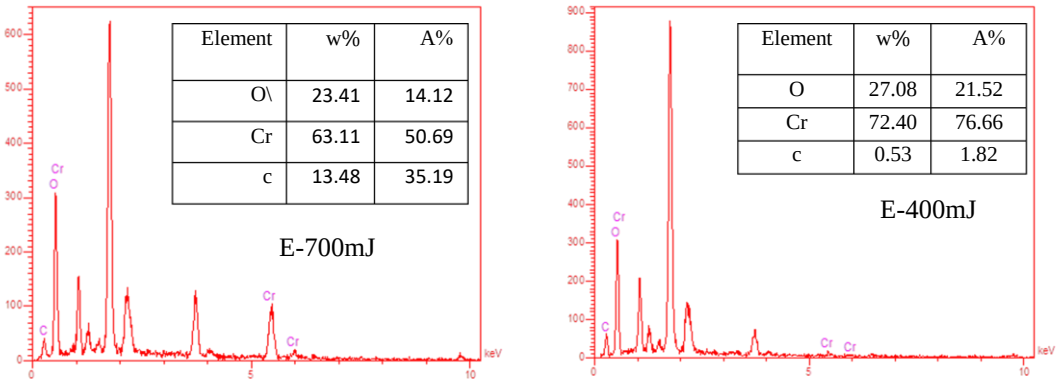

Figure 9: EDX Spectrum of Cr nanoparticles prepared at laser energies of 400 and 700 mJ

3.4 Antibacterial Activity of Cr NPs.

The effect of Cr nanoparticles produced by pulsed laser ablation on the activity of Staphylococcus aureus and Escherichia coli, a gram-positive and a gram-negative bacteria isolated from teeth was investigated. The Escherichia coli bacterial growth was affected by pulse laser energies of 400 mJ, 500 mJ, or 600 mJ. The higher energy of 700mJ was particularly effective ,as it resulted on clear cultures with bacterial growth . The bacteria count was 299×10^8 colony/ml before treatment. While the after treatment count number was 90×10^8 colony/ml with energy of 400mJ, 80×10^8 colony/ml with energy of 500mJ, 50×10^8 colony/ml with energy of 600mJ, and zero (no bacterial growth) at 700mJ energy, as shown in Figure 10. As for the effect of Cr nanoparticles produced by pulsed laser ablation on the activity of Staphylococcus aureus bacteria: before treatment, the bacterial count was 250×10^8 colony/ml. After treatment, it was reduced to 132×10^8 colony/ml for 400 mJ energy, 98×10^8 colony/ml for 500 mJ energy, 81×10^8 colony/ml for 600 mJ energy, and 60×10^8 colony/ml for 700 mJ energy, as shown in Figure 11. The killing rate of the two types of bacteria appears to be different. This could be due to the differences in the cell wall structure and composition of the two bacteria.

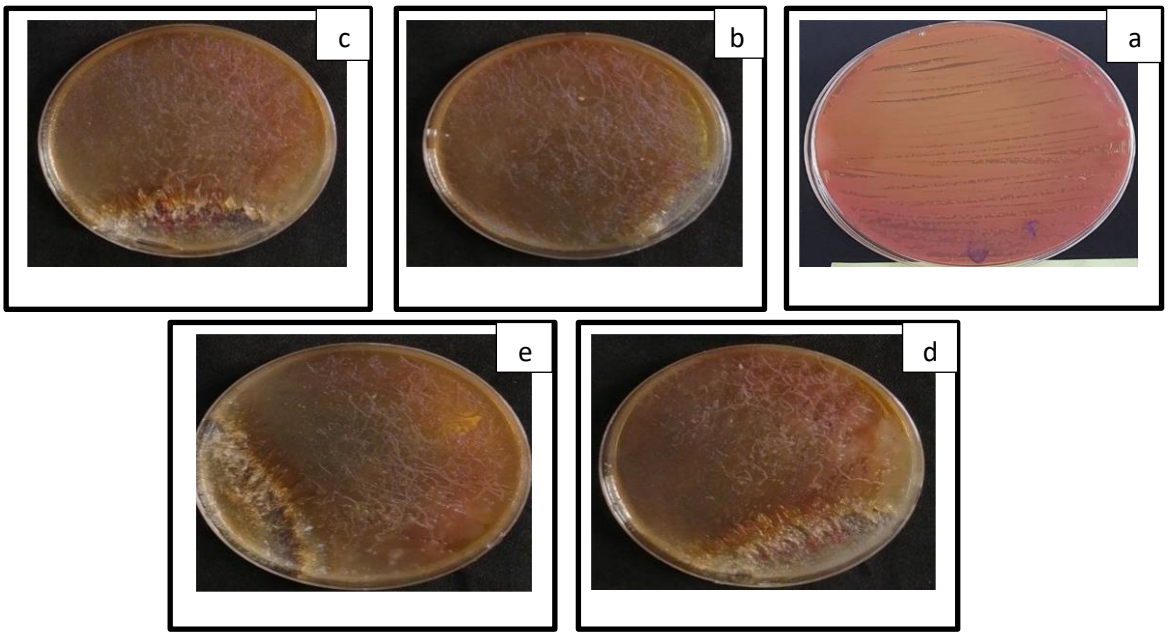

Figure 10: Antibacterial activity of Escherichia coli (a) before treatment. After treatment at (b) 400 mJ (c) 500mJ (d) 600mJ (e) 700mJ

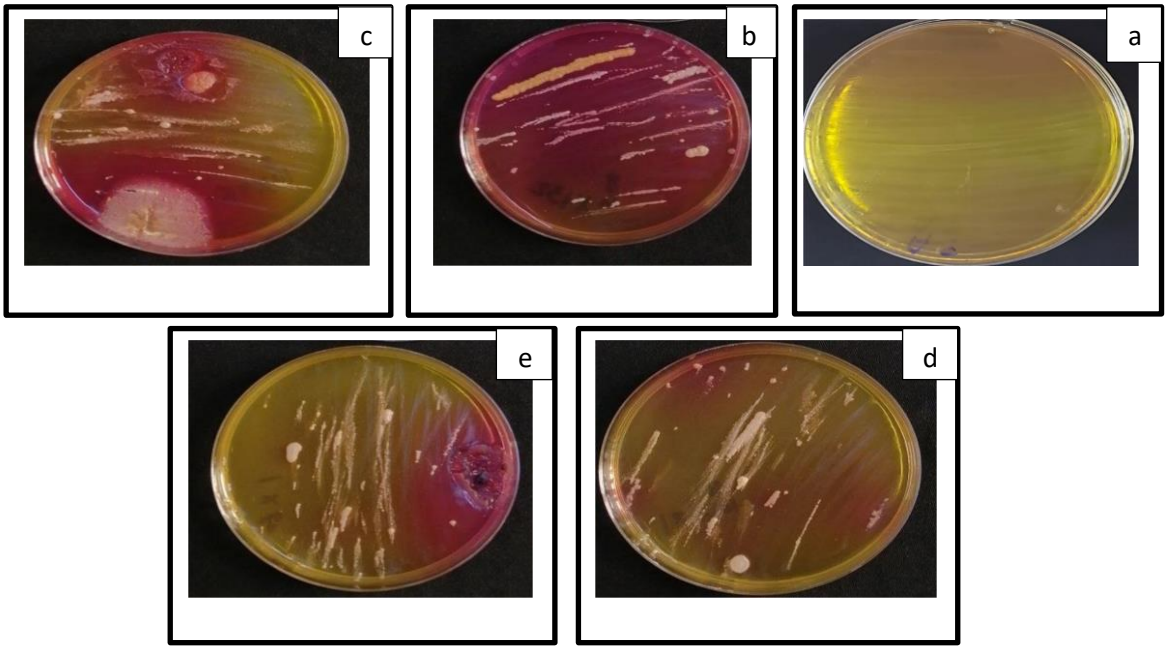

Figure 11: Antibacterial activity of Staphylococcus aureus (a) before treatment. After treatment at (b) 400 mJ (c) 500mJ (d) 600mJ (e) 700mJ

Figure (12) shows how bacteria colonies looked before and after treatment. There are several reasons for the killing process, taking into account the features of the bacteria; this includes the breakdown of biological processes caused by nanoparticles that are smaller than the size of the cell wall or cell membrane, and so they can enter the cell system[27,28].

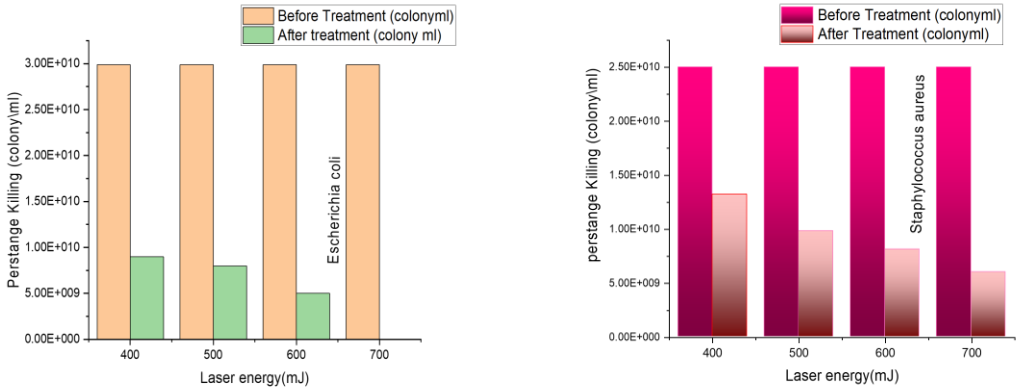

Figure 12: Histogram of antibacterial Activity at (400-700 mJ) showing the percentage killing by Cr NPs

Conclusions:

The study involved the production of chromium nanoparticles (Cr NPs) using laser-induced plasma at different pulse laser energies (400 - 700 mJ). XRD analysis showed that the Cr NPs had a crystalline structure, and their size increased with increasing the laser energy. FE-SEM analysis revealed that the Cr NPs formed were of spherical or semi-spherical morphologies. Atomic force microscopy (AFM) was used to study the molecular structure of the Cr NPs. The production of Cr NPs required different laser energies (400–700

mJ), which resulted in a range of bacterial death rates. The study found that Escherichia coli bacteria were completely eliminated with a laser energy of 700 mJ.

References:

[1] A. F. Ahmed, K. A. Aadim and A. A. Yousef, "Spectroscopic study of AL nitrogen plasma produced by DC glow discharge," *Iraqi Journal of Science*, vol. 59, no.1, pp. 494-501, 2018.

[2] A. A. Temur and A. F. Ahmed, "Investigation of the Electron Coefficients of (Ar, He, N2, O2) Gases in the Ionosphere," *Baghdad Science Journal*, vol. 19, no. 6, pp. 1558-1565, 2022.

[3] Q. A. Abbas, A. F. Ahmed, and F. A.-H. Mutlak, "Spectroscopic analysis of magnetized hollow cathode discharge plasma characteristics," *Journal of Optik*, vol. 242, p. 167260, 2021.

[4] A. F. Ahmed and A. A. Yousef, "Spectroscopic Analysis of DC-Nitrogen Plasma Produced using Copper Electrodes," *Iraqi Journal of Science*, vol. 62, no. 10, pp. 3560-3569, 2021.

[5] M.Tongmei, "Cavity ringdown laser absorption spectroscopy of free radicals," Thesis Online (HKUTO), University of Hong Kong, 2004.

[6] W.I. Yaseen, A.F .Ahmed, D. Al-Shakarchi and F.H Mutlak, "Development of a high-power LC circuit for generating arc plasma and diagnostic via optical emission spectroscopy&quot," *Journal Applied Physics*, vol. 128, no. 2, pp. 1-9, 2022.

[7] A. F. Ahmed, W. I. Yaseen, Q. A. Abbas, and F. A. H. Mutlak," Plasma treatment effect on SnO 2–GO nano-heterojunction: Fabrication, characterization and optoelectronic applications," *Applied Physics*, vol. 127, pp. 1–16, 2021.

[8] R. H. Jassim "Effect of (MnO, ZnO and Se) nanoparticles synthesized in liquid by laser induce plasma on thyroid," Thesis, College of Science, University Baghdad, 2020.

[9] F. A. H. Mutlak, M. Jaber, and H. Emad, "Effect of laser pulse energy on the characteristics of Au nanoparticles and applications in medicine," *Iraqi Journal of Science*, vol. 58, no. 4, pp.2364–2369 2017.

[10] M. A. Abed, F. A. H. Mutlak, A. F. Ahmed, U. M. Nayef, S. K. Abdulridha, and M. S. Jabir, "Synthesis of Ag/Au (core/shell) nanoparticles by laser ablation in liquid and study of their toxicity on blood human components," in *Journal of Physics: Conference Series* (IOP Publishing), vol. 1795, p. 012013, 2021.

[11] A. F. Ahmed, M. R. Abdulameer, M. M. Kadhim, and F. A.-H. Mutlak, "Plasma parameters of Au nano-particles ablated on porous silicon produced via Nd-YAG laser at 355 nm for sensing NH_3 gas," *Journal of Optik*, vol. 249, p. 168260, 2022.

[12] Q. K. Hammad, A. N. Ayyash, and F. A.-H. Mutlak, "Improving SERS substrates with Au/Ag-coated Si nanostructures generated by laser ablation synthesis in PVA," *Journal of Optics*, vol. 52, no. 1, pp. 1528–1536, 2023.

[13] M. V Allmen and A. Blatter, "*Laser-Beam Interactions with Materials: Physical Principles and Application*s," vol. 2, Springer Science & Business Media, 2013.

[14] N. A. Inogamov and Y. V Petrov, "Thermal conductivity of metals with hot electrons," *Journal of Experimental and Theoretical Physics*, vol. 110, pp. 446–468, 2010.

[15] T. S. Hussein, A. F. Ahmed, and K. A. Aadim, "Spectroscopic Analysis of CdO: Fe Plasma Generated by Nd: YAG Laser," *Iraqi Journal of Science*, vol. 63, no. 2, pp. 548-555, 2022.

[16] U. M. Nayef, A. J. Hadi, S. K. Abdulridha, F. A.-H. Mutlak, and A. F. Ahmed, "Tin dioxide nanoparticles synthesized via laser ablation in various liquids medium," *Journal of Optics*, vol. *52*, no. 1, pp. 1–8, 2022.

[17] T. S. Hussein and A. F. Ahmed, "Laser induced plasma of cadmium oxide: structural, morphological and optical properties," in *Journal of Physics: Conference Series* (IOP Publishing) , vol. 2114, no. 1, p. 12012, 2021.

[18] C. Jenul and A. R. Horswill, "Regulation of Staphylococcus aureus virulence, Microbiology spectrum," *Microbiol. Spectr*, vol. 7, no. 2, pp. 2–7, 2019.

[19] N. K. Abdalameer, "Spectroscopic Study of Plasma Parameters Produced by Different Methods to Synthesize ZnSe Nanoparticles For Medical Applications," Thesis College of Science for Women- University of Baghdad ,2021.

[20] T. A. Faiadh," Prepartion and Charastrization of PbO and PbS Nano-Thin films by Using Laser Ablation Method," Thesis ,College of Science for Women, University of Babylon, 2015.

[21] V. S. Jaswal, A. K. Arora, M. Kinger, V. D. Gupta, and J. Singh," Synthesis and characterization of chromium oxide nanoparticles," *Orient J Chem*, vol. 30, no. 2, pp.559–566 ,2014.

[22] J. Wang and S. Nie, "Application of atomic force microscopy in microscopic analysis of polysaccharide," *Trends in Food Science & Technology*, vol. 87, pp. 35–46, 2019.

[23] K. de Haan, Z. S. Ballard, Y. Rivenson, Y. Wu, and A. Ozcan, "Resolution enhancement in scanning electron microscopy using deep learning," *Scientific reports*, vol. 9, no. 1, pp. 1–7, 2019

[24] R. S. Mohammed, K. A. Aadim, and K. A. Ahmed, "Synthesis of CuO/ZnO and MgO/ZnO Core/Shell Nanoparticles with Plasma Gets and Study of their Structural and Optical Properties," *Journal of Modern Science*, vol. 8, no. 2, pp. 88-97, 2022.

[25] N. K. Abdalameer, S. N. Mazhir, and K. A. Aadim, "The effect of ZnSe Core/shell on the properties of the window layer of the solar cell and its applications in solar energy," *Energy Reports*, vol. 6, pp. 447–458, 2020.

[26] Y. Guo, G. Song, M. Sun, J. Wang, and Y. Wang, "Prevalence and therapies of antibiotic-resistance in Staphylococcus aureus," *Frontiers in cellular and infection microbiology*, vol. 10, p. 107 ,2020.

[27] M. A. Aswad, F. A. H. Mutlak, M. S. Jabir, S. K. Abdulridha, A. F. Ahmed, and U. M. Nayef, "Laser assisted hydrothermal synthesis of magnetic ferrite nanoparticles for biomedical applications," *Journal of Physics: Conference Series* (IOP Publishing), no.1, p.12030, 2021.

[28] R. A. Ismail, G. M. Sulaiman, S. A. Abdulrahman, and T. R. Marzoog," Antibacterial activity of magnetic iron oxide nanoparticles synthesized by laser ablation in liquid," *Materials Science and Engineering*, vol. 53, pp. 286–297, 2015.